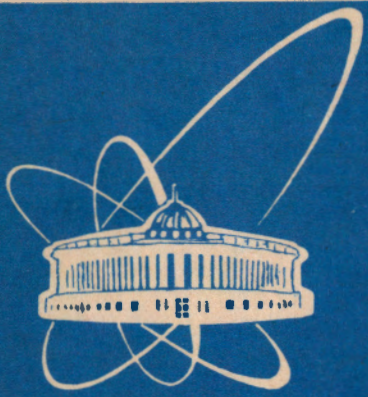

ОБЪЕДИНЕННЫЙ
ИНСТИТУТ
ЯДЕРНЫХ
ИССЛЕДОВАНИЙ

Дубна

E1-95-369

A.M.Taratin

DEFLECTION EFFICIENCY AND ENERGY LOSS DISTRIBUTIONS FOR HIGH ENERGY PROTONS IN A BENT CRYSTAL

Submitted to the Proceedings of the Workshop on Channeling and Other Coherent Crystal Effects at Relativistic Energies, Aarhus, July 10—14, 1995

1995

Таратин А.М.

E1-95-369

Эффективность отклонения и распределения ионизационных потерь энергии для протонов высокой энергии в изогнутом кристалле

Эффективность отклонения и распределения ионизационных потерь энергии протонов с энергией 450 ГэВ при прохождении через кристалл кремния, изогнутый вдоль (111) плоскостей, исследованы методом компьютерного моделирования. Выражение для тормозной способности, зависящее от пути частицы в кристалле, и локальная электронная плотность, усредненная вдоль траекторий частиц, использовались для расчёта спектров ионизационных потерь в рассматриваемых слоях кристалла. Показано, что наиболее вероятные потери энергии и страглинг для отклоненных частиц увеличиваются при прохождении участка кристалла с увеличивающейся кривизной. Характеристики рассчитанных спектров потерь энергии для отклоненной и неотклоненной кристаллом фракции пучка находятся в хорошем согласии с экспериментом.

Работа выполнена в Лаборатории высоких энергий ОИЯИ.

Препринт Объединенного института ядерных исследований. Дубна, 1995

1 Introduction

The energy losses of charged particles at their channeling in single crystals differ from the losses at random beam incidence when the particle directions are far from any axial or planar directions in the crystal. The positively charged particles being in channeling states move through the crystal regions with low electron density and their mean energy loss is usually smaller than for random incidence [1]. The crystal equiped with intrinsic surface barrier detectors allows to study particle states during their passage through the crystal by means of measurements of their energy losses [2, 3, 4]. The usage of the bent crystals and separation of the deflected beam fraction give an additional possibility to investigate the energy losses of well-channeled particles which possess low initial transverse energies at the crystal entrance avoiding the contribution from randomly traveling particles [5].

In this work deflection efficiency and energy loss distributions of 450 GeV protons during their passage through the (111) bent silicon crystal have been considered by computer simulation. The path dependent stopping power and local electron density averaged along the particle trajectories were used to construct the energy loss distributions for the considered crystal layers. The calculated energy loss distributions for deflected and undeflected beam fractions are in good agreement with the recent experimental results [5]. It was shown that with the beam penetration into the crystal the most probable energy loss and straggling increase for the deflected fraction at the crystal part with increasing curvature.

2 Calculation model

The particle trajectories in a bent crystal were calculated in the same manner as it was made us earlier [6]. That is the particle motion in the effective potential of the bent atomic planes was considered, and the change in transverse velocity of the particle due to multiple scattering by the crystal electrons and nuclei was performed at every trajectory step whose value was much smaller than the spatial period of particle oscillations in the channel. The model takes into account the realistic distribution of the electron density in the crystal and good discribes the particle dechanneling in the straight and bent crystal [6]. The full crystal length was divided into layers with thickness $S_L = 2.5$ mm to consider the evolution of energy loss spectra of protons during their passage through the crystal.The

path dependent stopping power [7]

$$\mu(x) \equiv \frac{dE}{ds}(x) = \frac{2\pi Z_1^2 e^4}{mv^2}\{[NZ_2 + \rho(x)][\ln\frac{2mv^2\gamma^2}{I} - \beta^2] + C(x) - NZ_2\delta\}, \quad (1)$$

$$C(x) = \sum_{K_x \neq 0} \rho(K_x) e^{iK_x x} \ln(2mI/\hbar^2 K_x^2) \quad (2)$$

was used to calculate the mean energy loss for every particle in the considered crystal layer

$$\bar{\Delta}_{tr} = \frac{dE}{ds}(\rho_{tr}, C_{tr})\, S_L, \quad (3)$$

where C(x) is the correction taking into account inhomogeneity of the electron density and the crystal structure periodicity, $\rho(K_x)$ is the Fourier transform of the electron density $\rho(x)$ averaged along the considered crystal planes, K_x is the reciprocal-lattice vector, δ is the density effect correction, I is the mean excitation potential of the crystal atoms, ρ_{tr}, C_{tr} are the values of electron density and correction averaged along the particle trajectory in the layer.

The mean energy loss $\bar{\Delta}_{tr}^j$ and averaged electron density ρ_{tr}^j for the j-particle in the layer were used to construct the Landau distribution $\varphi(\lambda_{ij})$, where λ_{ij} is the distribution parameter value for the considered value of the particle energy loss Δ_i

$$\lambda_{ij} = \frac{\Delta_i - \bar{\Delta}_{tr}^j}{\xi^j} - \beta^2 - 0.423 - \ln(\xi^j/T_{max}), \quad (4)$$

$$\xi^j = \frac{2\pi e^4}{mv^2}\rho_{tr}^j S_L. \quad (5)$$

The width of the j-particle Landau distribution is proportional to the averaged electron density ρ_{tr}^j. Therefore, to make the weight of every particle the same as for random particles the normalization of the distribution was made

$$\tilde{\varphi}(\lambda_{ij}) = \frac{NZ_2}{\rho_{tr}^j}\varphi(\lambda_{ij}). \quad (6)$$

The array of energy loss values for particles in the crystal layer $\Delta_i = i\,\Delta_s$, where Δ_s is the distribution step, was considered. The energy loss distribution in the layer was calculated by summation over all N particles

$$F(\Delta_i) = \sum_{j=1}^{N} \tilde{\varphi}(\lambda_{ij}). \quad (7)$$

Fig.1 shows the averaged electron density (a), the C(x) correction term (b), and the mean energy loss of 450 GeV protons (c) in the (111) channels of a silicon crystal at the room

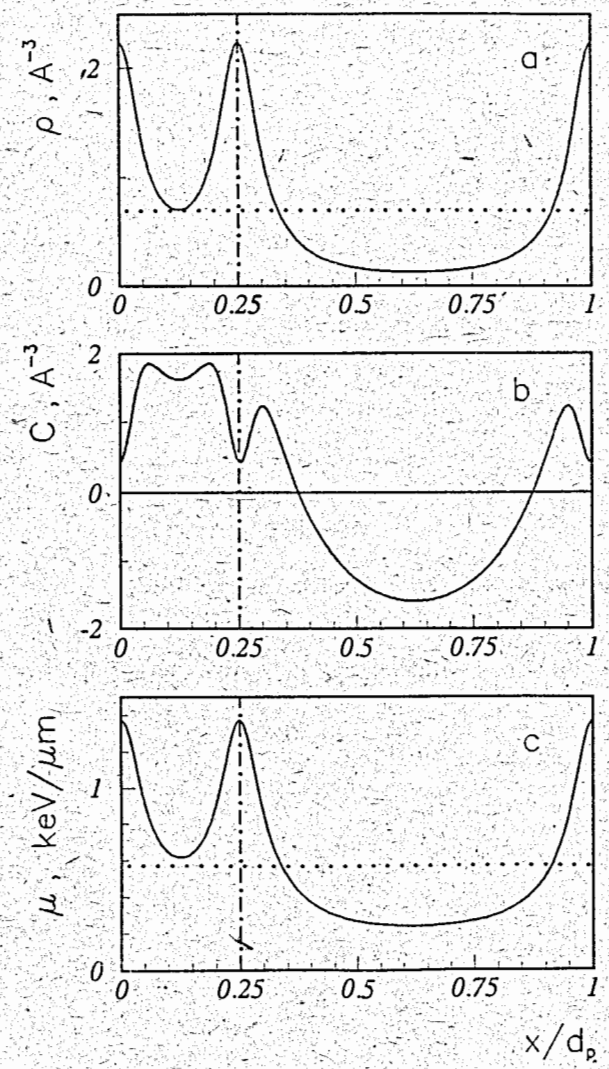

Fig.1. The averaged electron density (a), the C(x) correction term (b), and the mean energy loss of 450 GeV protons (c) in the (111) channels of a silicon crystal at the room temperature in the Moliere approximation as a function of the distance from the atomic plane. The dotted lines show the corresponding values for random case. The dot-dashed lines separate the narrow and wide channels.

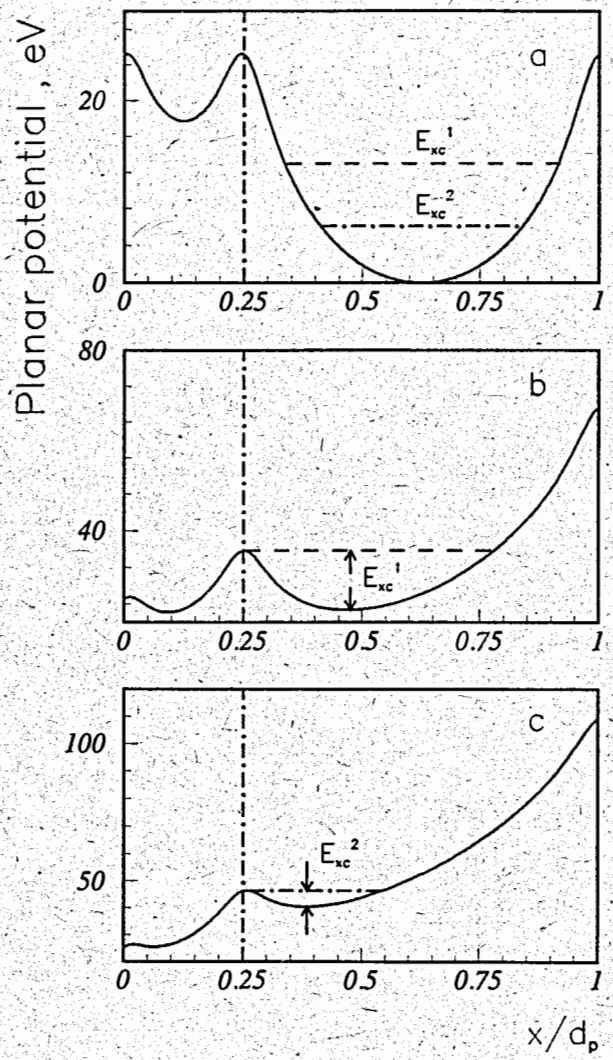

Fig.2. The continuum potential of the (111) silicon channel (a), and the effective planar potential for the crystal bent with the average curvature (b) and with the maximum one (c) at the bending angle of 8.9 mrad. The critical transverse energies of particles E_{xc}^1, E_{xc}^2 for the wide channels in the bent crystal are shown by the dashed and dot-dashed lines, accordingly, in fig.2b and fig.2c. The same values of E_{xc} in the straight channel potential are shown in fig.2a.

temperature in the Moliere approximation as a function of the distance from the atomic plane. Both the electron density and the correction behaviour lead to the decrease of the mean energy loss for particles moving in the wide channels and the increase in the narrow ones in comparison with the loss at the random incidence.

In the experiment [5] the Si crystal 50 mm long in beam direction was bent with a 3-point bending device. So, a 10 mm long straight part was at each end of the crystal. The crystal bend produced by the bending device is non-uniform with maximum curvature near the central point. The same crystal shape was considered in our simulation. It was assumed that the crystal curvature increases linearly with approach to the central point

$$\kappa(s) = \begin{cases} \kappa_m \, 2s/L, & s \leq L/2, \\ \kappa_m \, (2 - 2s/L), & s > L/2, \end{cases}$$

where $\kappa_m = 2\,\kappa_o$ is the maximum curvature, $\kappa_o = 1/\mathrm{R}_o = \alpha/\mathrm{L}$ is the average curvature which is created when the central crystal part with the lenght L is uniformly bent with the angle α.

Fig.2 shows the continuum potential of the (111) silicon channel (a), and the effective planar potential for the crystal bent with the average curvature (b) and with the maximum one (c) at the bending angle of 8.9 mrad. The critical transverse energy of particles for channeling decreases with increasing the crystal curvature. So, there is no possibility for channeling in the narrow channels for this bend of the crystal at its central point, fig.2c. The critical transverse energy values of E_{xc}^1, E_{xc}^2 for the wide channels are shown in fig.2b,c. These values allow to estimate approximately the part of the W-channeled particles at the crystal entrance, see fig.2a, which can be kept in the channels during the passage through the bent part of the crystal.

3 Deflection efficiency

The beam deflection efficiency by a bent crystal is determined by the capture probability of the incident beam particles into the channeling regime and the dechanneling rate of the captured fraction during its passage through the crystal. The capture depends on the beam divergence. At the crystal bending the capture reduces due to decreasing the depth of the effective planar potential. The particle dechanneling in the straight crystal occurs mainly due to multiple scattering by the crystal electrons and nuclei. In the bent crystal

when its curvature increases along the crystal length the captured particles can leave the channels due to bending or centrifugal dechanneling, which is caused by gradual lowering the potential barrier. The crystal bending gives a good possibility to study the particle dechanneling due to the space unfolding of the process.

The computer simulation of the 450 GeV proton beam passage through the silicon crystal bent along the (111) atomic planes was performed at the same bending angles of the crystal as in the experiment [5]. It was supposed that the angular distribution of the incident beam is Gaussian with the rms angular deviation ϑ. Fig.3a,b show the angular distributions of the beam passed the crystal for the bending angles of 1.4 and 8.9 mrad, accordingly, for the case with the 3-point bending device. Fig.3c is the same as fig.3b for the case when the central crystal part is uniformly bent. The distributions consist of two peaks for the straight beam and for the deflected fraction. There are also particles between these peaks. They are the particles which were initially channeled at the crystal entrance but then lost in the bent part of the crystal. It is clearly seen for the bigger bending angle that the particles leave bent channels mainly in the crystal part where its curvature increases. The particle losses occur here mainly due to the bending dechanneling.

The computer simulation allows to register exactly the particle states in the crystal. The particles which carry out a finite transverse motion in the narrow or wide channels of the crystal will be called N- or W-channeled particles below. Fig.4,5 show the dependences of N-channeled and W-channeled fractions on the crystal depth, accordingly, for the same conditions as fig.3. Besides, curve 2 in fig.4,5a shows the fraction captured into the channeling states in the crystal volume. The volume capture events occur mainly in the front straight part of the crystal because its bend takes away fast the plane directions out of the narrow incident beam.

The N-channeled fraction begins decrease noticeably in the front straight part of the crystal already. It occurs due to ordinary multiple scattering by the crystal electrons whose density is higher in the narrow channels than the average one. The centrifugal dechanneling which appears in the bent crystal part with increasing curvature completes the process for the large bending angle, fig.4b. For small bending angles when the centrifugal dechanneling is not strong about few percents of the N-channeled particles achieve the exit end of the crystal, fig.4a.

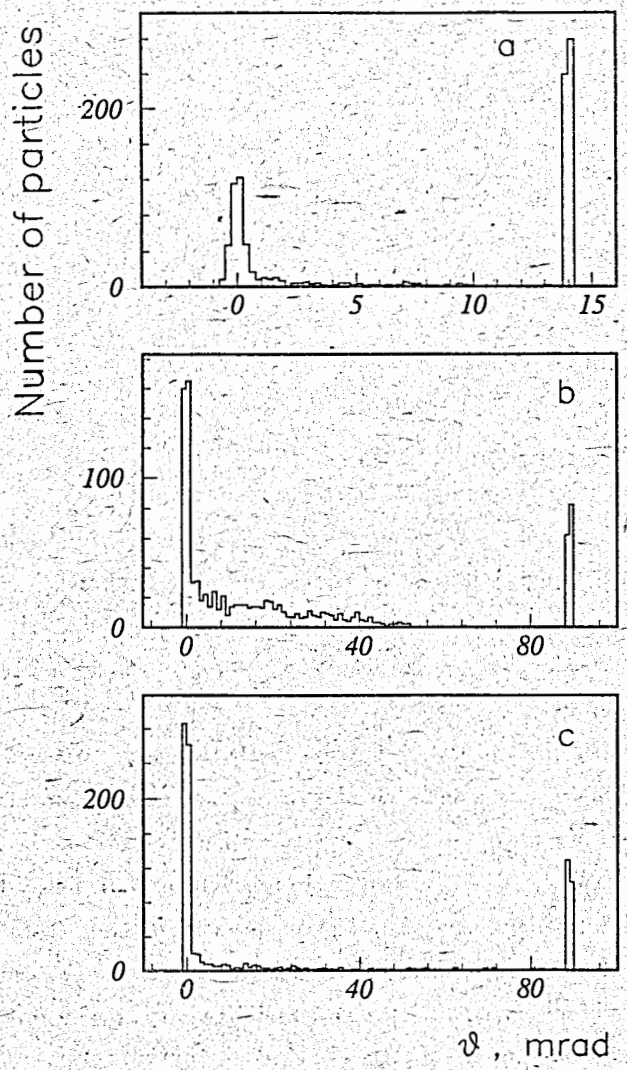

Fig.3. The angular distributions of the beam passed the crystal for the case with a 3-point bending device, the bending angles 1.4 (a) and 8.9 mrad (b). (c) - for the case when the central crystal part is uniformly bent, $\alpha = 8.9$ mrad.

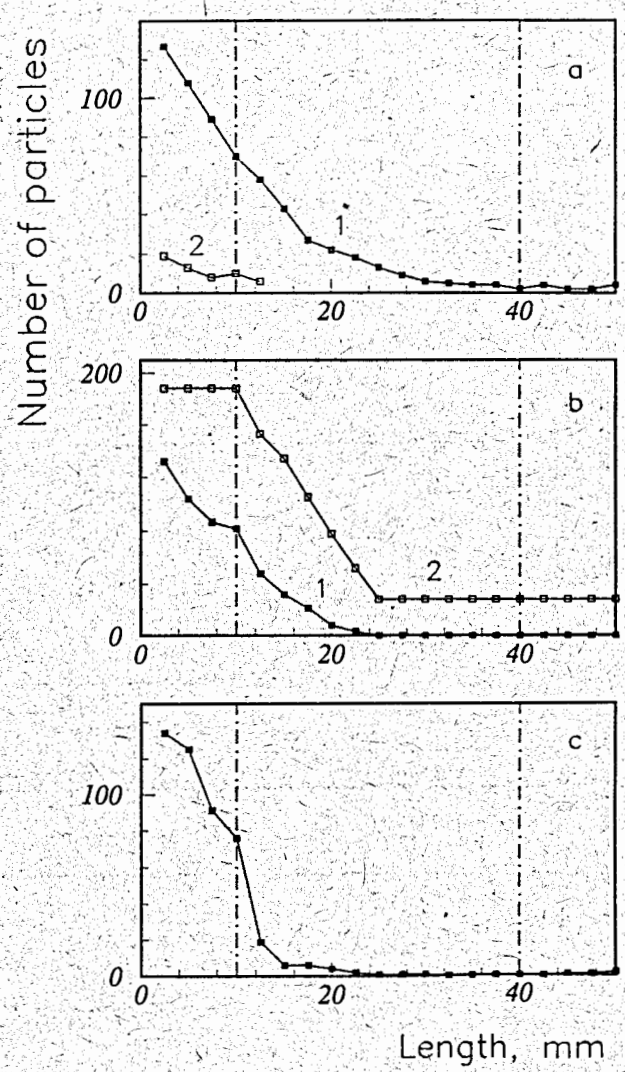

Fig.4. The dependence of the particle fraction which are in the channeling states in the narrow (111) channels of the silicon crystal on the crystal depth. The conditions are the same as for fig.3. (a) - curve 2 is the fraction captured into the channeling regime in the crystal volume. (b) - curve 2 for the idealized case when multiple scattering was switched off. The dot-dashed lines show the straight parts at the crystal ends.

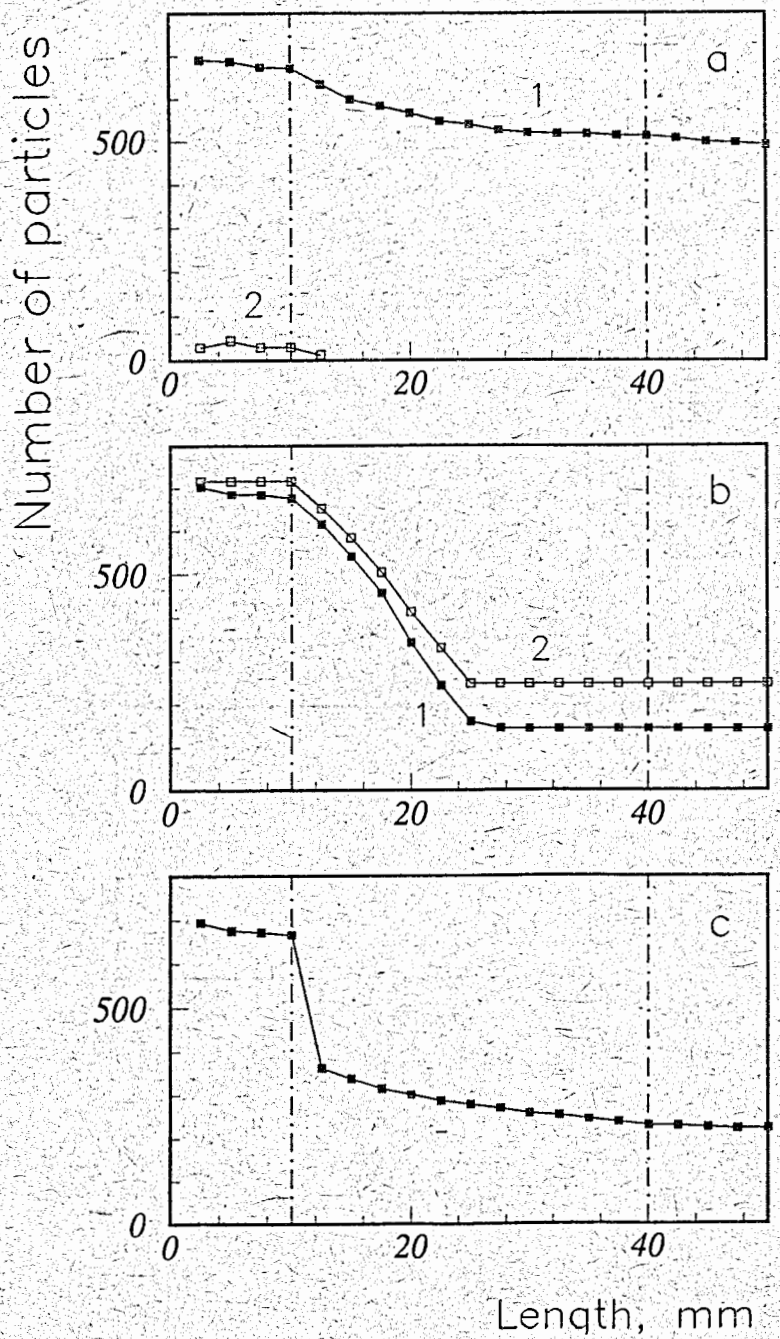

Fig.5. The same as fig.4 for the wide (111) channels.

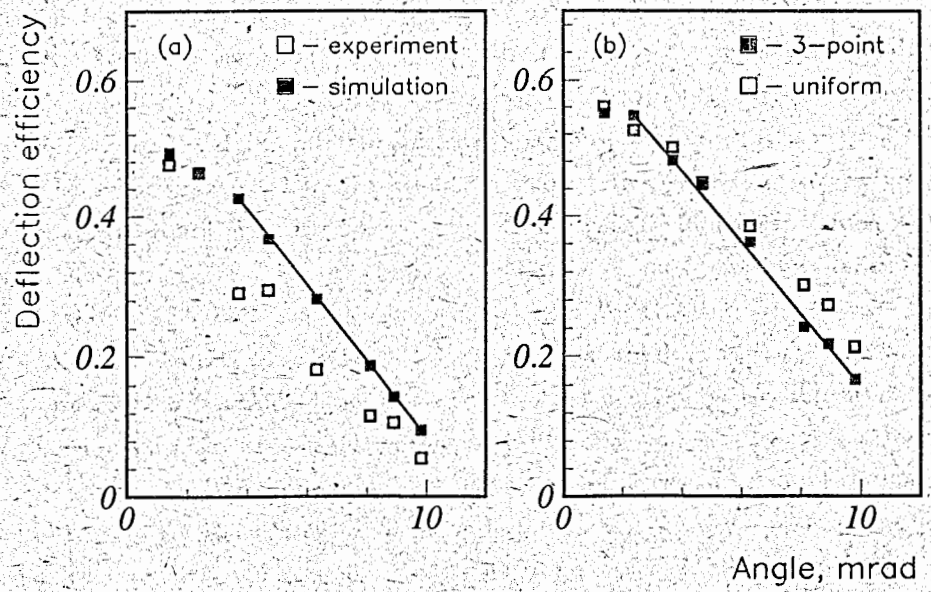

Fig.6. The deflection efficiency of 450 GeV proton beam with a silicon crystal bent along the (111) planes as a function of the crystal bending angle. (a) Comparison of the experimental results with the simulation ones when a 3-point bending device is used, the rms angular deviation of the beam $\bar{\vartheta} = 3$ μrad. (b) The simulation results for two cases when a 3-point bending device is used, and when the central crystal part is uniformly bent, $\bar{\vartheta} = 1$ μrad.

For the W-channeled fraction the ordinary dechanneling in the straight parts is small because of low electron density in the middle of the wide channels, but the fraction decreases fast in the first bent part of the crystal, fig.5b. Curve 2 in fig.4,5b shows the idealized case when multiple scattering was switched off. It is seen by comparison these curves that the centrifugal dechanneling is the main process of the particle losses out of the channels for the large bending angles. On the other hand, in the second bent part of the crystal the losses of the W-channeled fraction are almost absent because the potential depth is growing up to the previous level of the straight channel, whereas the transverse energies of the particles passed the central crystal point are limited by the lowest value of the barrier of the effective potential which exists in this point. In the case when the central crystal part is uniformly bent, fig.4,5c, the centrifugal dechanneling occurs only in one point at the transition from the front straight crystal part to the bent one, but these losses are very large.

The calculated deflection efficiency as a function of the crystal bending angle is presented in fig.6. For small bending angles the efficiency values calculated for the beam with the rms angular deviation $\theta = 3$ μrad are close to the experimental ones, whereas for the large angles they are noticeably higher, fig.6a. This discrepance may be caused by additional losses of the channeled particles in the experiment due to local distortions of the crystal lattice from the pressure of the bending device. The beam deflection efficiency for the large bending angles is considerably higher for the case when the central crystal part is uniformly bent, curve 2 in fig.6b, $\bar{\vartheta} = 1$ μrad.

4 Energy loss spectra of protons in bent crystal

The energy loss spectrum for a random beam incidence which is a usual Landau distribution is shown in fig.7a. Fig.7b shows the energy loss distribution in the first crystal layer for the aligned incidence of 450 GeV proton beam, $\bar{\vartheta} = 3$ μrad, the beam tilt angle relative to the plane direction $\vartheta_o = 0$. There are two peaks in the spectrum at $\Delta^1_{mp} \simeq 0.6\Delta^R_{mp}$ and $\Delta^2_{mp} \simeq 1.18\Delta^R_{mp}$, where Δ^R_{mp} is a most probable energy loss for random incidence of the beam. The first peak is formed by the W-channeled particles with low transverse energies. The second one by the N-channeled particles, and the W-channeled particles with large transverse energies, and besides the quasi-channeled particles which are governed by the

average planar potential too, but move through the crystal crossing the atomic planes at small angles. Their straggling is 54 % larger than for random incidence due to high local electron density along their trajectories.

The energy loss spectrum of the deflected beam fraction for the crystal bending angle of 1.4 mrad is also shown in fig.7b. The deflected particles form low-energy-loss side of the peak I. They are the W-channeled particles with sufficiently low transverse energies to keep in the channels during the passage through the central point of the crystal where the depth of the effective planar potential is minimum and considerably smaller than for straight channels.

The spectra of the deflected fractions for two bending angles of the crystal, 1.4 amd 8.9 mrad, are compared in fig.7c. The spectrum width is reduced by 30-35 % for the bigger angle because the deflected particles have lower initial transverse energies and, consequently, smaller electron density along the trajectories, what reduses the energy loss straggling.

Fig.8 shows the evolution of the energy loss spectra for the deflected and undeflected beam fractions during the passage through the bent crystal. The energy losses for the undeflected particles of group II become the same as for random incidence soon after the particle entrance into the bent crystal part because of dechanneling and fast leaving the angular region near the planes due to their bending. On the other hand, the energy losses for the deflected fraction increase during their approach to the central crystal point because of increasing the trajectory shift to the outer channel wall where the electron density is higher. The same occurs with the undeflected particles of group I, which were initially W-channeled. The growth of the energy losses for the deflected beam fraction in the crystal part with increasing curvature is more clearly shown in fig.9, where the energy loss spectra for different crystal depths are combined.

Fig.10 shows the aligned energy loss spectra for the cases when the incident beam inclines relative to the direction of the crystal planes (a), and when its divergence increases (b). In the both cases the channeled fraction decreases. The decrease of the W-channeled fraction is observed in reducing the spectrum maximum I, whereas the decrease of the particle fraction whose energy losses are larger than the random one leads to the shift of the maximum II to the lower values of the energy losses. On the other hand, the most probable energy loss of the W-channeled group I increases with disorientation of the

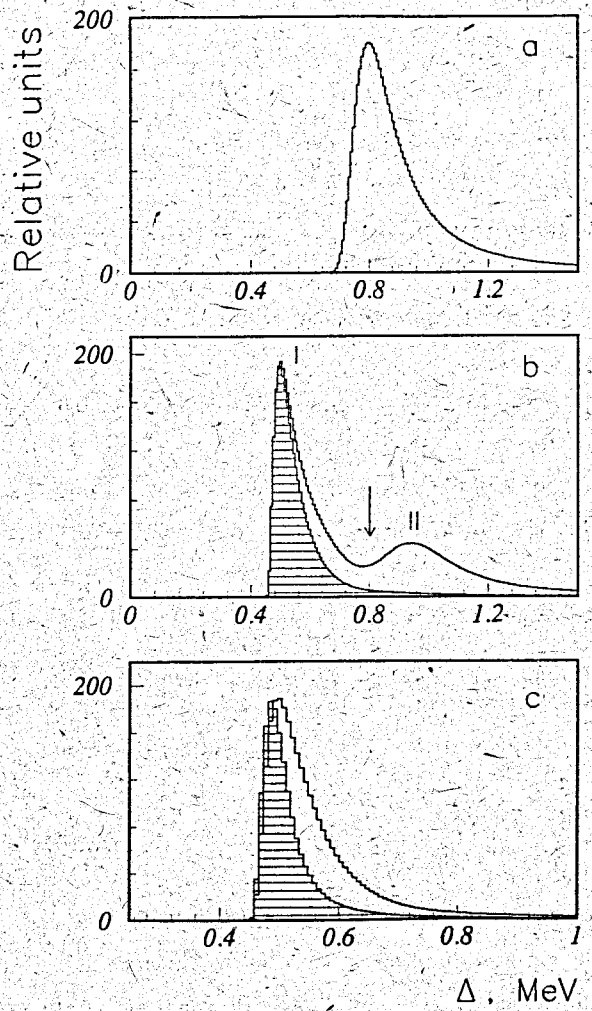

Fig.7. The energy loss distributions in the first crystal layer for random incidence (Landau distribution) (a) and for aligned incidence of 450 GeV proton beam, the rms angular deviation of the beam $\bar{\vartheta} = 3$ μrad (b). The hatched histogram is the distribution for the deflected beam fraction at the crystal bending angle of 1.4 mrad. The arrow shows the most probable energy loss for the random incidence. (c) Comparison of the deflected fraction distributions for two bending angles of the crystal, 1.4 and 8.9 mrad (hatched). The distributions were normalized at the same height.

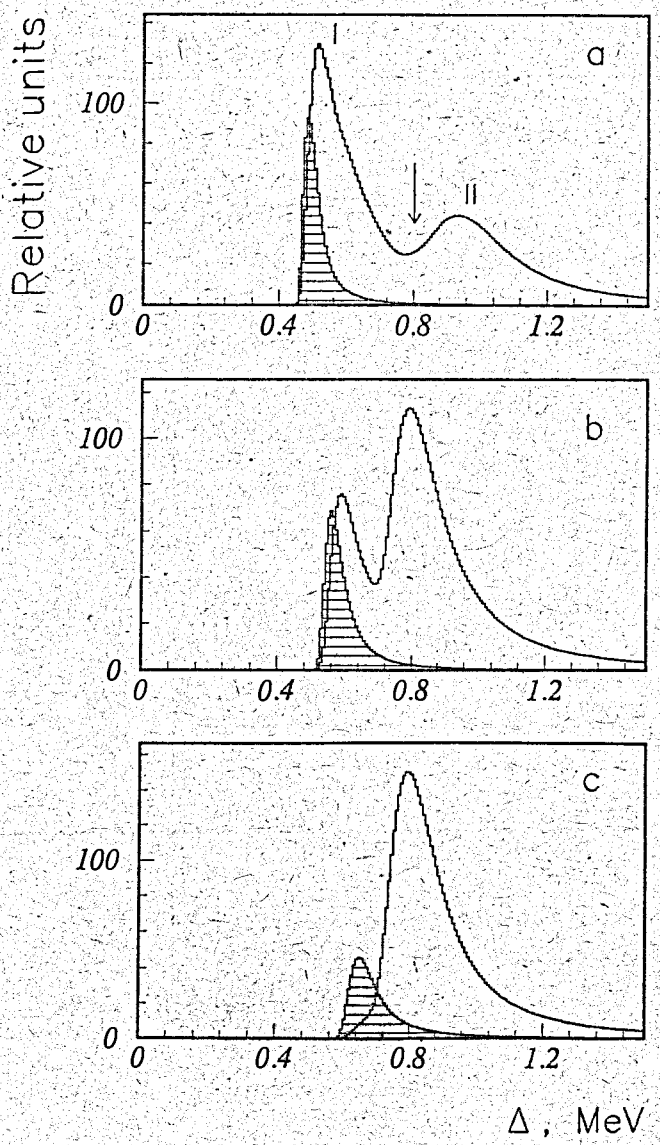

Fig.8. The evolution of the energy loss spectra for the deflected (hatched) and undeflected beam fractions during the passage through the bent crystal, the crystal bending angle is 8.9 mrad. The spectra are shown for the crystal layers: 1 (a), 8 (b), 10 (c).

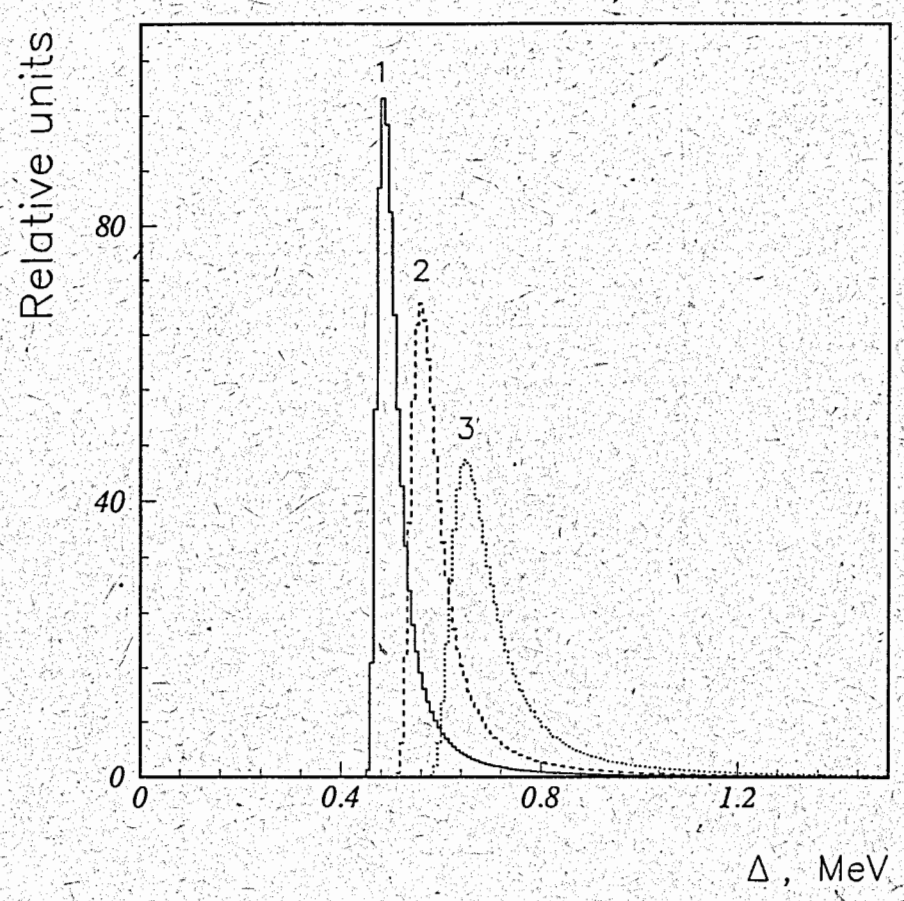

Fig.9. The energy loss spectra of the deflected beam fraction for the different crystal depths, in the layers: 1 (1), 8 (2), 10 (3). The crystal bending angle $\alpha = 8.9$ mrad.

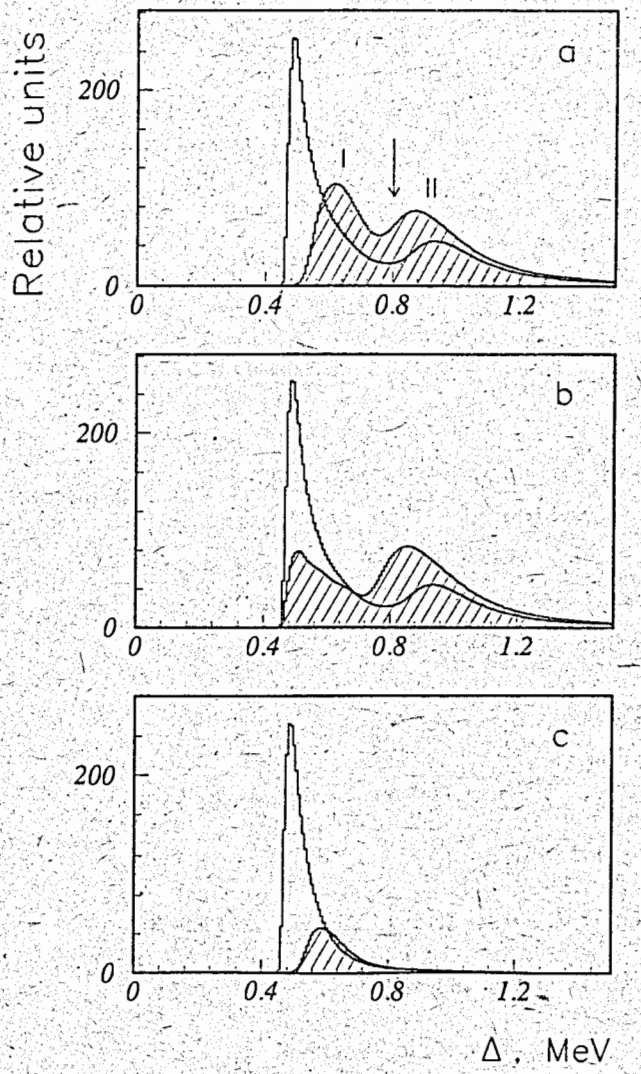

Fig.10. The aligned energy loss spectra (a) for the different beam tilt angles relative to the crystal plane direction, $\vartheta_o = 0$ and 7 μrad (hatched), $\vartheta = 1$ μrad; (b) for the different beam divergence, $\vartheta = 1$ and 10 μrad (hatched), $\vartheta_o = 0$. (c) The energy loss spectra for the deflected fraction of the beam, the conditions are the same as for fig.10a.

crystal with the beam and does not change with increasing the beam divergence. The corresponding growth of the most probable energy loss for the deflected fraction with the crystal-beam disorientation is shown in fig.10c. This growth occurs because the higher levels of the transverse energies are inhabited by the beam particles.

5 Conclusion

The calculated energy loss distributions for the deflected and undeflected beam fractions in the (111) silicon bent crystal, naimely their maximum positions and widths, are in good agreement with the experiment [5]. The computer experiment showed that the most probable energy loss and straggling of the deflected beam fraction increase during the beam penetration in the crystal part with increasing curvature.

The position of the energy loss spectrum maximum for channeled particles is determined by their transverse energy distribution. It was demonstrated by our computer simulation that the most probable energy loss for the deflected fraction of the narrow incident beam grows with increasing the beam tilt angle relative to the crystal planes and does not change with increasing the beam divergence.

References

[1] J. Lindhard, K. Dan. Vidensk Selsk. Mat. Fys. Medd. 34 (1965).

[2] H. Esbensen et al., Phus.Rev. B18 (1978) 1039.

[3] V.A. Andreev et al., Pis'ma Zh.Eksp.Teor.Fiz. 36 (1982) 346.

[4] J.F. Bak et al., Nucl.Phys. B242 (1984) 1.

[5] S.P. Moller et al., Nucl.Instr.Meth. B84 (1994) 434.

[6] A.M. Taratin and S.A. Vorobiev, Nucl.Instr.Meth. B47 (1990) 247.

[7] H. Esbensen and J. Golovchenko, Nucl.Phys. A298 (1978) 382.

Рукопись поступила в издательский отдел
10 августа 1995 года.